swiss medical weekly

Original article | Published 03 January 2024 | doi:https://doi.org/10.57187/s.3503
Cite this as: Swiss Med Wkly. 2024;154:3503

Influenza transmission dynamics quantified from RNA in wastewater in Switzerland

Sarah Nadeau[ab], Alexander J. Devaux[c], Claudia Bagutti[d], Monica Alt[d], Evelyn Ilg Hampe[d], Melanie Kraus[e], Eva Würfel[e], Katrin N. Koch[f], Simon Fuchs[e], Sarah Tschudin-Sutter[g], Aurélie Holschneider[c], Christoph Ort[c], Chaoran Chen[ab], Jana S. Huisman[ab], Timothy R. Julian[c], Tanja Stadler[ab]

[a] Department of Biosystems Science and Engineering, ETH Zurich, Basel, Switzerland
[b] Swiss Institute of Bioinformatics, Lausanne, Switzerland
[c] Department of Environmental Microbiology, EAWAG, Dübendorf, Switzerland
[d] State Laboratory of Basel-Stadt, Basel, Switzerland
[e] Department of Health, Canton of Basel-Stadt, Basel, Switzerland
[f] Cantonal Office of Public Health, Department of Economics and Health, Canton of Basel-Landschaft, Liestal, Switzerland
[g] Division of Infectious Diseases and Hospital Epidemiology, University Hospital Basel and University of Basel, Basel, Switzerland

Summary

INTRODUCTION: Influenza infections are challenging to monitor at the population level due to many mild and asymptomatic cases and similar symptoms to other common circulating respiratory diseases, including COVID-19. Methods for tracking cases outside of typical reporting infrastructure could improve monitoring of influenza transmission dynamics. Influenza shedding into wastewater represents a promising source of information where quantification is unbiased by testing or treatment-seeking behaviours.

METHODS: We quantified influenza A and B virus loads from influent at Switzerland's three largest wastewater treatment plants, serving about 14% of the Swiss population (1.2 million individuals). We estimated trends in infection incidence and the effective reproductive number (R_e) in these catchments during a 2021/22 epidemic and compared our estimates to typical influenza surveillance data.

RESULTS: Wastewater data captured the same overall trends in infection incidence as laboratory-confirmed case data at the catchment level. However, the wastewater data were more sensitive in capturing a transient peak in incidence in December 2021 than the case data. The R_e estimated from the wastewater data was roughly at or below the epidemic threshold of 1 during work-from-home measures in December 2021 but increased to at or above the epidemic threshold in two of the three catchments after the relaxation of these measures. The third catchment yielded qualitatively the same results but with wider confidence intervals. The confirmed case data at the catchment level yielded comparatively less precise R_e estimates before and during the work-from-home period, with confidence intervals that included one before and during the work-from-home period.

DISCUSSION: Overall, we show that influenza RNA in wastewater can help monitor nationwide influenza transmission dynamics. Based on this research, we developed an online dashboard for ongoing wastewater-based influenza surveillance in Switzerland.

Prof. Dr Tanja Stadler
ETH Zürich, Department of Biosystems Science and Engineering (D-BSSE)
Schanzenstrasse 44
CH-4056 Basel
tanja.stadler[at]bsse.ethz.ch

Introduction

Detection and monitoring of influenza outbreaks are crucial but challenging tasks. Reporting systems for influenza-like illness and laboratory-confirmed influenza infections are used to monitor temporal trends in influenza transmission [1]; to estimate the number of symptomatic cases, hospitalizations, and deaths due to influenza [2]; and to help hospitals and public health officials plan vaccination campaigns and allocate treatment resources [3]. For example, doctors may prescribe influenza-specific treatment based on knowledge of an ongoing influenza outbreak in the region and a symptomatic diagnosis before waiting for laboratory confirmation [4], underscoring the public health relevance of accurate detection and monitoring of influenza outbreaks.

The coronavirus disease 2019 (COVID-19) pandemic has severely impacted existing influenza surveillance systems based on clinical/syndromic data. First, COVID-19 and influenza share many symptoms, complicating symptom-based influenza diagnosis [5]. Test-seeking behaviour also changed during the pandemic, reportedly increasing compared to pre-pandemic in the U.S. [2]. Finally, pandemic-related public health measures and associated behavioural changes have disrupted typical seasonal influenza transmission dynamics [6–7]. Therefore, pandemic-related changes have simultaneously changed influenza transmission dynamics and decreased the reliability of ongoing influenza surveillance efforts. Consequently, many influenza surveillance reports include COVID-19-related disclaimers about the representativeness and interpretability of the data [2, 8, 9]. In summary, the emergence of COVID-19 as a new endemic disease necessitates adjustments to existing influenza surveillance programs moving forward.

Wastewater surveillance represents a promising alternative method for pathogen surveillance that is independent of testing behaviour, can indicate the relative incidence of pathogens responsible for influenza-like illnesses, and can capture unreported cases [10]. Infected individuals shed many pathogens via their stool and sputum and/or from their skin, depending on the pathogen. Therefore, pathogen particles can enter the wastewater when infected individuals use the toilet, brush their teeth, or shower. Previous studies have shown that various pathogens are detectable in wastewater samples [11–12]. In regions where household wastewater is centrally collected, wastewater represents a pooled community sample, and wastewater pathogen loads indicate community disease burden. The idea of wastewater-based epidemiology is not new but has recently experienced a surge in popularity, with many communities developing detection and monitoring strategies for severe acute respiratory syndrome coronavirus 2 (SARS-CoV-2) in wastewater [13].

Wastewater-based surveillance offers the opportunity to better understand influenza dynamics, similar to its role in understanding COVID-19 dynamics. Wolfe et al. [14] established that influenza A virus (IAV) particles in wastewater correlated well with incidence rates from two well-characterized outbreaks on U.S. university campuses. Mercier et al. [15] similarly quantified IAV particles in wastewater at the municipality scale in Ottawa, Canada. They established that IAV concentrations in wastewater correlated well with municipal surveillance data when lagged 17 days, meaning wastewater was an early indicator of transmission dynamics in this system. They also extended wastewater surveillance by sub-typing the detected IAV. Most recently, Boehm et al. [7] developed a multiplexed method to quantify influenza A and B alongside several other respiratory viruses in wastewater. They confirmed that IAV concentrations in wastewater at the municipal level were associated with laboratory-confirmed cases at the state level. Influenza B virus (IBV) concentrations were low and frequently undetectable. These previous studies indicate that IAV is detectable in wastewater and can be used to study transmission dynamics in the community.

In this study, we aimed to implement wastewater surveillance for influenza at the national level in Switzerland and estimate influenza A and influenza B virus transmission dynamics from wastewater. We measured the concentrations of seasonal influenza types A and B at Switzerland's three largest wastewater treatment facilities, which together serve approximately 14% of the Swiss population (1.2 million individuals), from December 2021 to April 2022. Following a previously established method, we deconvoluted wastewater influenza loads to estimate trends in infection incidence and the effective reproductive number (R_e). We compared the wastewater-based results with laboratory-confirmed infection incidence in each catchment area. We have continued to measure influenza A and influenza B virus concentrations in these catchments since October 2022. The results presented here, and the results of our ongoing monitoring efforts, are available on an online dashboard at https://wise.ethz.ch/influenza/. All the analysis and dashboard code is open-source. We anticipate that these results and resources will help inform public health officials and hospitals about the onset and intensity of future influenza seasons.

Methods

Quantifying influenza RNA in wastewater

Twenty-four-hour flow-composite samples from raw influent wastewater were collected at Swiss wastewater treatment facilities in Zurich (ARA Werdhölzli), Geneva (STEP Aïre), and Basel (ProRheno AG). Twice on weekends, 48-hour flow-composite samples were taken in Basel rather than the regular 24-hour samples. The respective catchment areas for these facilities are shown in figure 1. Mean hydraulic residence times are 1 hour in the Zurich catchment and 1.5 hours in the Basel catchment. Residence time is unknown for the Geneva catchment but is expected to be similar to Zurich and Basel. Travel distances to the treatment facilities are also similar (0.2–15 km for Zurich, 0.5–11 km for Basel, and 0.1–19.1 km for Geneva) [16].

For the Zurich and Geneva facilities, total nucleic acid was extracted from 40 ml of wastewater using a modified version of the Wizard® Enviro Total Nucleic Acid Kit (Promega Corporation, Madison, WI, USA). Nucleic acids were eluted in 80 µl of RNAse/DNAse-free water and further purified using a OneStep PCR Inhibitor Removal Kit (Zymo Research, Irvine, CA, USA). Nucleic acid extracts were stored at –80°C for up to a year before analysis. For the Basel facility,samples were stored at 4°C for up to 72 hours before further processing. Total nucleic acids were concentrated and extracted from 40 ml of wastewater using the Maxwell® RSC Environ Wastewater TNA Kit (Promega Corporation). Nucleic acid extracts were stored at –20°C for up to two weeks and at –80°C for up to a year before analysis.

All samples were collected within the scope of ongoing wastewater-based SARS-CoV-2 surveillance projects [17–18]. We retrospectively quantified influenza A and influenza B viruses from stored RNA extracts for this study. For the Zurich and Geneva samples, IAV and IBV were quantified using digital reverse transcription polymerase chain reactions (RT-dPCR) with 5.4 µl of wastewater RNA extract. The RT-dPCR procedure is described in the Supplemental Methods. At least two replicate aliquots from, on average, two samples per week were analyzed. For the Basel facility,IAV and IBV were quantified using a triplex one-step quantitative reverse transcription polymerase chain reactions (RT-qPCR) with 5 µl of wastewater RNA extract and the GoTaq® Enviro FluA/FluB /SARS-CoV-2 System (Promega Corporation) according to the protocol provided in the manual. Single aliquots from, on average, two samples per week were analyzed. After quantification, we converted the IAV and IBV concentrations in genome copies per mL to daily pathogen loads (genome copies per day) by multiplying the concentration measurements by the total inflow to the respective wastewater treatment facility on the sample date.

Estimating trends in influenza incidence and Re from wastewater

We used our previously developed approach to estimate trends in infection incidence and the effective reproductive

number from pathogen RNA in wastewater [19]. The actual estimation was done using the estimateR package for the R statistical software [20], which implements the R_e estimation method of Cori et al. [21]. R_e is the expected number of secondary infections caused by a single infectious individual at a specific time. This metric is commonly used for monitoring disease transmission dynamics, particularly because there is an easily interpretable epidemic threshold at $R_e = 1$ that indicates whether an outbreak is expected to grow ($R_e > 1$) or decline ($R_e < 1$). R_e estimates also put wastewater- and case-based metrics on a common scale. R_e can vary over time according to population immunity, infection control measures, and behavioural changes.

First, we scaled the wastewater load data by the treatment plant-specific minimum detected load (1.6×10^{11} for Zurich, 1.1×10^{11} for Geneva, and 3×10^{9} for Basel), which assumes that the minimum detected load represents one infected individual. Such an assumption is necessary to make the range of wastewater measurements comparable to the incidence in an outbreak since the deconvolution method used is optimized for case data and does not perform well when inputs are orders of magnitude higher (as with wastewater loads) [19]. As a sensitivity analysis, we also attempted using 10× and 100× scaling (i.e. the minimum detected viral load corresponds to 10 or 100 infected individuals in the catchment rather than 1).

Next, we performed linear interpolation to generate a regular daily time series of measurements. We chose linear interpolation because cubic spline interpolation produced spurious lows due to day-to-day oscillations in the wastewater measurements. We also used locally estimated scatterplot smoothing (LOESS) to smooth the time series. Briefly, locally estimated scatterplot smoothing generates a smooth curve by combining polynomial regression models fit to localized subsets of the data. By interpolating and smoothing, we implicitly assume that true influenza incidence in a catchment does not change greatly day-to-day and that temporal noise in wastewater measurements comes from other factors such as variation in laboratory processing and detection methods, differing residence time in the sewers depending on the source, biofilm sloughing, or stochastic noise associated with temporally varying inputs [22–23].

We estimated R_e from the interpolated, smoothed wastewater measurements using the "get_block_bootstrapped_estimate" function in R's estimateR package [20]. This function estimates R_e in two steps. The first step back estimates infection incidence from observations (in our case, wastewater RNA load measurements) via deconvolution using a distribution that characterizes delays from infection to observation. Following Huisman et al. [19], we used a pathogen-shedding load distribution, which characterizes how individuals shed virus particles into wastewater over the course of their infections. The second step estimates R_e from deconvoluted infection incidence using the method of Cori et al. [21]. This method requires assuming a distribution for how infectious individuals are over the course of their infections, which in practice is approximated by a serial interval distribution. The R_e inference procedure assumes that the serial interval, the pathogen shedding load distribution, and the ascertainment probability for an influenza RNA molecule in wastewater do not vary through time.

For the main results, we assume a gamma shedding load distribution with a mean of 2.5 days and a standard deviation of 1 day (empirical median: 2.4 days) based on virus

Figure 1: Catchment area map. Coloured areas show the catchment areas of the three wastewater treatment facilities where influenza A and B virus loads were measured. The Basel facility serves several communities in France (Neuwiller) and Germany (Weil-Otterbach and Inzlingen) that are not shown. The community of Brüglingen in Münchenstein, served by the Basel facility, is also not shown.

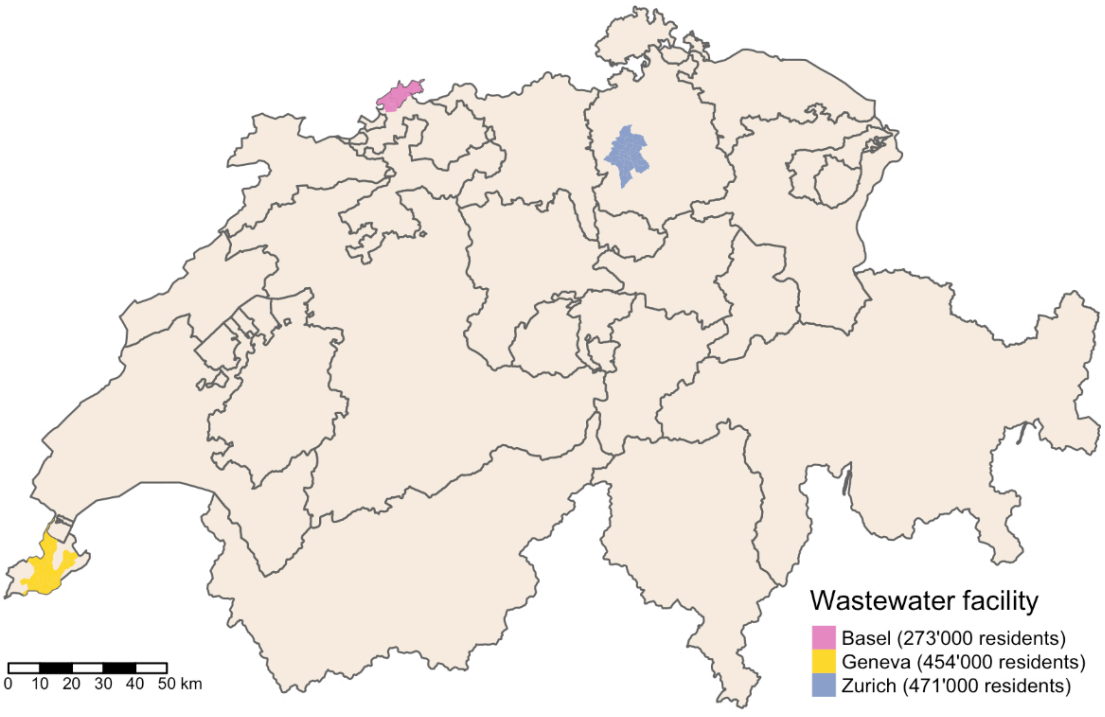

load measured in respiratory samples [24] (see the Supplemental Methods for details). As a sensitivity analysis, we also attempted a gamma distribution based on virus load measured in faecal samples [25–26], with a mean of 12.2 days and a standard deviation of 7.6 days (empirical median: 10.7 days). The distributions' fit to viral load data are shown in figure S1. Delays inside the sewer system to reach the wastewater sample collection point were assumed to be negligible. For the R_e estimation step, we assumed influenza cases had a serial interval with a mean of 2.6 days and a standard deviation of 1.5 days based on Ferguson et al. [27].

Uncertainty in the infection incidence deconvolution was accounted for by performing 500 block-bootstrap replicates of the measurement error, as described in Huisman et al. [19]. Uncertainty in the R_e estimation, which is reported as the 95% credible interval for R_e, was combined with the uncertainty across the bootstrap replicates for infection incidence, which is reported as the 95% bootstrap confidence interval (the estimateR option "combine_bootstrap_and_estimation_uncertainties"). We accounted for both estimate and measurement uncertainty by using the union of the highest of each type of uncertainty.

Comparison to other influenza surveillance data

The Federal Office of Public Health (FOPH) collects data on influenza cases in Switzerland in two ways. First, general practitioners participating in the sentinel system "Sentinella" report the number of consultations for influenza-like illness, a syndromic diagnosis, each week. Swabs from a selection of these influenza-like illness cases are tested for influenza. Second, diagnostic laboratories must report any laboratory-confirmed case of influenza to the Federal Office of Public Health, regardless of patient symptoms or whether the practitioner participates in the Sentinella system [8].

To access the Sentinella data, we downloaded national influenza-like illness incidence from the Federal Office of Public Health's influenza website [8]. The weekly influenza positivity rate among tested swabs from influenza-like illness cases was estimated by digitizing figure 4 from the 2021/22 Sentinella report [28] using the online tool https://automeris.io/WebPlotDigitizer/. We corrected influenza-like illness incidence for the time-varying positivity rate by multiplying each week's influenza-like illness incidence by the estimated positivity rate for that week. Next, we received the number of laboratory-confirmed influenza cases ("confirmed cases") reported by diagnostics laboratories to the Federal Office of Public Health. We only received laboratory-confirmed cases from postal codes in the catchment areas of studied wastewater treatment plants. The Federal Office of Public Health provided these data stratified by week, influenza type, and postal code from 24 August 2021. Some of the postal codes are only partially served by the studied wastewater treatment plants. Therefore, we scaled the number of cases from these postal codes by the fraction of the total postal code area included in the wastewater treatment plant's catchment area based on delineating the catchment boundaries. This approach assumes cases were uniformly distributed across the postal code's geographic area. We directly compared the wastewater data to the resulting number of laboratory-confirmed cases per catchment area. We note that confirmed cases were also reported outside of our study period; in this article, we only consider data from 1 December 2021 to 30 April 2022.

We calculated R_e estimates from the catchment-level confirmed case data using the same procedure as for the wastewater data, except that cubic spline (rather than linear) interpolation was used to estimate daily cases from the weekly reported data using the "cubicspline" function from R's pracma package [29]. We also used a delay distribution based on a timeline of symptom severity rather than viral shedding based on the assumption that the probability of an individual consulting a doctor or seeking a test is associated with their symptom severity, with most individuals getting tested on the day of their peak symptoms. We generated this distribution by fitting a gamma distribution to data from Carrat et al. [24], resulting in a distribution with a mean of 4.5 days from infection and a standard deviation of 0.8 days (empirical median: 3.4 days; see the supplemental methods and figure S1 in the appendix).

Results

During the period from 1 December 2021 to 30 April 2022, we detected influenza A virus particles in the wastewater on more than 90% of sampled days: influenza A virus was detected on 37/38 days from Zurich, 39/42 days from Geneva, and 45/50 days from Basel. The influenza B virus was detected less often in wastewater: influenza B virus was detected on 7/35 days from Zurich, 9/33 days from Geneva, and 1/50 days from Basel (figure 2 and figure S2 in the appendix). The wastewater load data and confirmed case data by catchment area suggest one or more IAV outbreak peaks in each catchment (figure 2A). However, the wastewater and confirmed case data only robustly supported an IAV peak occurring roughly between March and May 2022 across all three catchments. Combining the confirmed case data across all postal codes for which we received this data shows a smaller peak in cases around January 2022, but the March-May 2022 peak dominates (figure S3 in the appendix). The national influenza-like illness data had three atypical peaks across the 2021/22 season (figure 2B). For comparison, influenza-like illness incidence during the entire 2021/22 season was much lower than in pre-COVID-19 pandemic Swiss influenza seasons [28]. Only the peak in March-May 2022 remained when the influenza-like illness data was adjusted for influenza positivity over time (figure 2B).

We could compare catchment-specific influenza outbreak dynamics based on wastewater data and laboratory-confirmed case data by deconvolving both the wastewater loads and case data at the catchment level to estimate trends in infection incidence. We could align incidence estimates on a comparable time scale by applying the appropriate delay distribution to each data type (figure 3). There were two notable points in this analysis. First, the magnitude of wastewater-based infection incidence estimates was sensitive to the scaling of wastewater loads. Our scaling based on the assumption that the minimum detected load corresponds to a single infected individual should be conservative, meaning infection incidence is likely higher than reported here, because we assume the minimum correspondence between wastewater loads and infections in

the catchment (a single infected individual). Second, since there were very few laboratory-confirmed cases of influenza B virus during the study period, we only show case-based results for influenza A virus. There were six confirmed IBV cases in the Geneva catchment and none in the Zurich or Basel catchments. In comparison, there were 965 confirmed IAV cases in the Geneva catchment, 359 in the Basel catchment, and 255 in the Zurich catchment (figure S3 in the appendix). Similarly, we do not report results for IBV in Basel wastewater since it was only detected on one day.

The estimated trends in infection incidence derived from the wastewater data show strong evidence of an influenza A virus outbreak in Zurich, Geneva, and Basel in December 2021; this outbreak was not robustly observed in the confirmed case data (figure 3). The same trend is also evident in the raw wastewater load data (figure 2). This outbreak observed in wastewater appears to have peaked around the same time measures were introduced to reduce population mobility and contacts in Switzerland to combat the spread of the Omicron variant of SARS-CoV-2 (table 1). Around the time measures were lifted (first half of February), wastewater-based estimates indicate that influenza A virus incidence again increased in all three catchments. Confirmed influenza A virus infections also increased during this period.

Influenza B virus incidence was estimated to be much lower than influenza A virus incidence in the Zurich and Geneva catchments, consistent with the many fewer confirmed IBV cases than IAV cases observed. The wastewater data provide very weak support for a small peak in IBV infections in Geneva around the time mobility restrictions were introduced and in Zurich around the time they were lifted. However, these results were based on detecting low IBV concentrations in only a few samples on a handful of days (figure 2 and figure S2 in the appendix).

We note that infection incidences for both IAV and IBV generally shift over time, depending on the assumed shedding load distribution. All estimates shifted 1–2 weeks further to the past with a shedding load distribution based on potentially longer faecal shedding rather than respiratory shedding (figure S4 in the appendix). However, the qualitative correspondence between the wastewater-based estimates and mobility restriction measures remained.

Next, we used the effective reproductive number (R_e) to obtain further insight into the epidemic dynamics. R_e helps us confidently identify when influenza outbreaks are growing or declining (when confidence bounds on R_e exclude the epidemic threshold of 1). We note that R_e estimates are comparably robust to different scalings of the wastewater load data, at least up to differences of several orders of magnitude, since they are only based on relative changes in incidence over time (figure S5). Regarding the incidence estimates, the timing of the R_e estimates depends on the chosen shedding load distribution (figure S4).

Figure 4 shows that for the influenza A virus in Zurich and Geneva, the wastewater-based R_e decreased to around or below the epidemic threshold of 1 (confidence interval below 1.05) in mid-December 2021. Mobility restriction measures in Switzerland were strengthened considerably on 20 December 2021 to combat the Omicron variant of SARS-CoV-2 (table 1). The same decreasing trend in R_e around this time was observed in the wastewater-based R_e from Basel, although confidence intervals were wider

Figure 2: Influenza measurements from wastewater versus typical surveillance data. (A) The two data sources used to estimate Re. Wastewater measurements (in blue) are shown as the mean (points) and range (error bars) of measurements across aliquots from each sampled day. Days on which no aliquots had detectable virus are shown with crossed rather than round points. Note that wastewater quantification methods differed between the Zurich and Geneva catchments and the Basel catchment. Laboratory-confirmed cases (in red) are shown as a line connecting weekly reported cases within the catchment. (B) The weekly national incidence of influenza-like illness (ILI; in orange) and the same values corrected for weekly percent influenza positivity among tested influenza-like illness swabs (in brown).

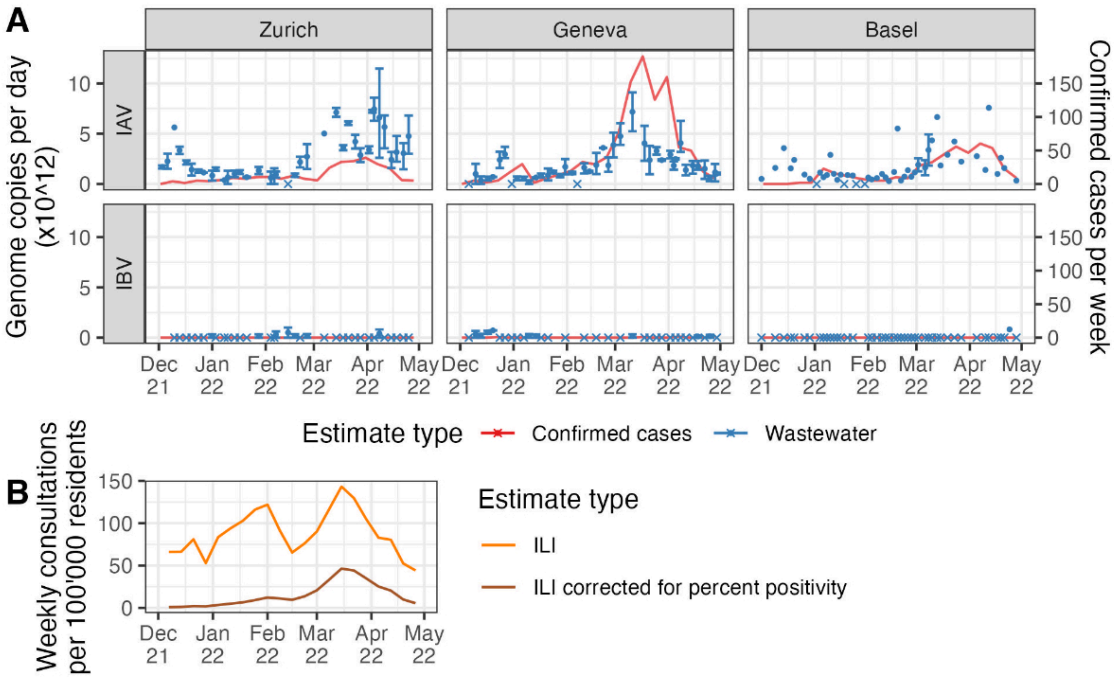

around the epidemic threshold. Later, R_e was around or above 1 (confidence interval above 0.97) in the Zurich and Geneva catchments in the period after the relaxation of the measures. Assuming less conservative scalings for wastewater loads increased the certainty of these R_e estimates, pushing the lowest values significantly below 1 and the highest values significantly above 1 (figure S5 in the appendix).

Confirmed influenza A virus cases in each catchment were very low for most of the sample period, causing the delayed start of R_e estimates and large confidence intervals for case-based estimates in figure 4. We also have confirmed case data for postal codes corresponding to several other catchment areas where we only started wastewater surveillance after the 2021/22 season. In most catchments, confirmed cases showed a similar peak in March-May 2022 as in the Zurich, Geneva, and Basel catchments, and R_e estimates based on catchment-level confirmed cases generally declined after March 2022. However, case numbers were low in these other smaller catchment areas (figure S3), so trends are more stochastic (figure S6 in the appendix). Combining all confirmed cases from all postal codes for which we had data yielded a R_e estimate indicating R_e was above 1 in Switzerland in early March 2022 (figure S6). However, even combining all available case data, case-based R_e estimates were still too uncertain in December 2021 to draw any conclusions. Therefore, the wastewater-based R_e estimates are more precise than confirmed-case-based estimates, at least at the catchment level.

Figure 3: Trends in infection incidence. Infection incidence estimates are based on a deconvolution from wastewater influenza measurements (blue) or laboratory-confirmed influenza A cases in each catchment (red). Coloured bands show the 95% bootstrap confidence interval for each estimate. Note that the magnitude of wastewater-based estimates is sensitive to the scaling of wastewater loads and that true incidence is likely higher than shown here (see the main text). Influenza B case numbers were too low to run the estimateR pipeline on. Shaded areas show when work-from-home measures were in place, and dashed lines show the start and end dates of stronger measures to limit gathering sizes and require COVID-19 certificates and masks in more situations to combat the Omicron variant of SARS-CoV-2 (see table 1).IAV: influenza A virus; IBA: influenza B virus.

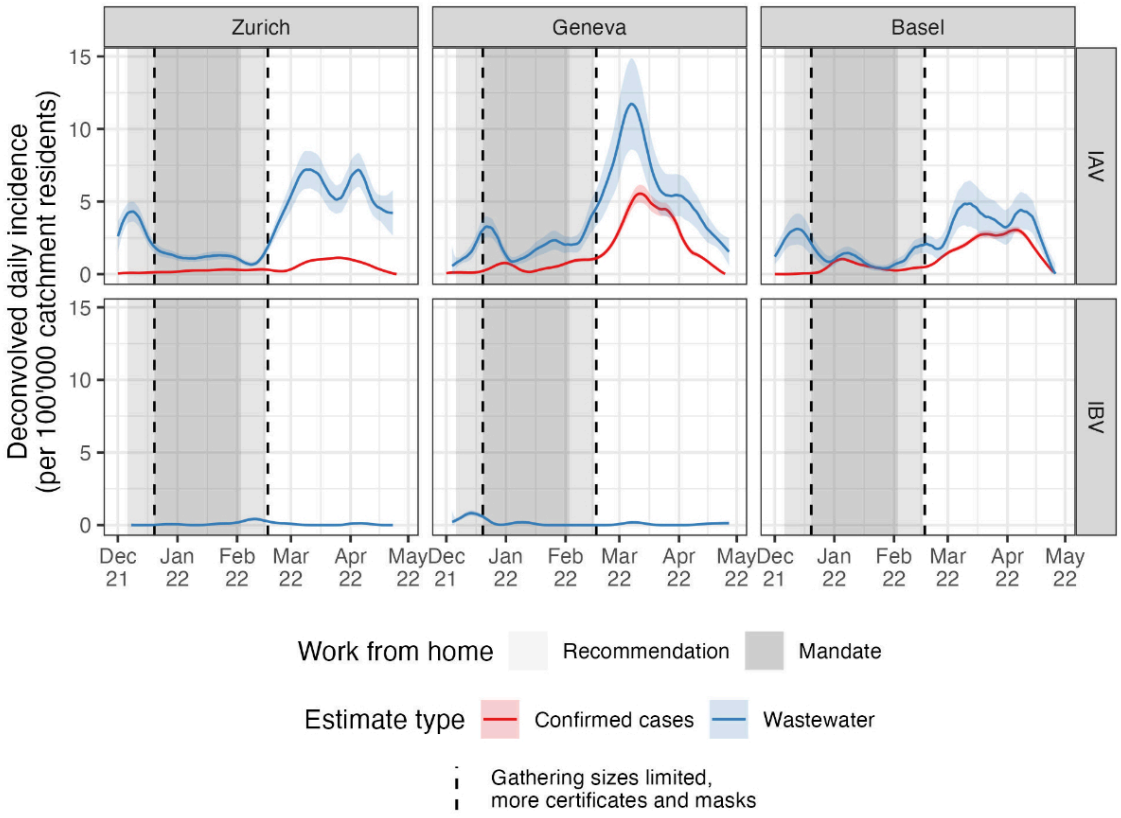

Table 1:
The selected measures used to combat the Omicron variant of SARS-CoV-2 in Switzerland. The table only shows the major measures used to reduce population mobility and contacts; a complete list of measures is available on the Federal Office of Public Health website [30].

Start date	End date	Measure	Source
6 Dec 2021	17 Feb 2022	Work-from-home recommendation.	Federal Office of Public Health [30]; Swissinfo.ch [31]
20 Dec 2021	3 Feb 2022	Work-from-home mandate.	Federal Office of Public Health [30]
20 Dec 2021	17 Feb 2022	Gathering size was limited; COVID certificates and masks were required in more situations.	Swissinfo.ch [31]
17 Feb 2022	30 Mar 2022	None except isolation of individuals with a positive test and masks in public transit and health care settings.	Swiss Federal Council [32]

The incidences of influenza B virus based on wastewater and confirmed cases were too low to generate reliable R_e estimates (figure S6).

All these results are available on an online dashboard at https://wise.ethz.ch/influenza/. At the time of manuscript revision, ongoing monitoring results were available through June 2023. Generally speaking, higher influenza A and influenza B virus wastewater loads and case numbers during the 2022/23 season resulted in narrower confidence intervals for R_e than in the 2021/22 season, with R_e roughly peaking around 1 December 2022 across the studied catchments (figure S7 in the appendix).

Discussion

In this study, we presented proof-of-concept results for quantifying influenza transmission dynamics based on wastewater viral loads. We were able to estimate trends in infection incidence and quantify the effective reproductive number for the influenza A virus in the three largest wastewater catchment areas in Switzerland. The influenza B virus was occasionally detectable in these catchment areas but at low concentrations. Altogether, these data provide a contrasting perspective on influenza outbreak dynamics to the confirmed case data, with the wastewater-based dynamics qualitatively aligning better to population mobility restrictions in winter 2021/22 due to the Omicron variant of SARS-CoV-2 than confirmed case data at the same geographic scale (catchment areas). Moving forward, we plan to expand our wastewater-based surveillance project to include additional catchment areas for which we have laboratory-confirmed case data (figure S3), which will enable further validation of the trends observed in this proof-of-concept project.

A primary limitation of this study, and indeed of general wastewater-based pathogen surveillance, is that pathogen shedding, transport through the sewershed, and decay dynamics in wastewater are poorly understood. Depending on the specific pathogen and sewershed characteristics, these dynamics likely vary between pathogen types and wastewater catchments. We rescaled wastewater loads to incidence values using the minimum detected wastewater viral load in each catchment for our specific R_e estimation method. This scaling depends both on the detection limit of our quantification method and the specific sewershed. Therefore, we cannot compare the absolute magnitudes between the wastewater- and confirmed case-based incidence estimates shown in figure 3, nor can we compare these magnitudes for wastewater-based incidence across catchments. Since the proportion of influenza cases ascertained via the Sentinella system was estimated to be around 5% in Switzerland [33], the laboratory-confirmed case-based incidence estimates in figure 3 are likely significant underestimates, as are the wastewater-based estimates at the scaling used. However, relative incidence should be comparable across influenza types (IAV and IBV) within the same catchment. In contrast, R_e estimates are comparable across catchments and pathogen types since they are based on relative changes through time.

We performed several sensitivity analyses to test the robustness of our results to unknown influenza dynamics in wastewater. First, we showed that R_e estimates are robust to several orders of magnitude difference in the scaling of wastewater loads, except that confidence intervals become arbitrarily small when the scaling results in higher incidence estimates (figure S5). The scaling we used provided comparably conservative (wide) confidence intervals. Then, we also performed a sensitivity analysis for the shedding load distribution, accounting for faecal versus respiratory influenza shedding. This analysis showed that the magnitude of our incidence and R_e estimates were generally robust to unknown shedding dynamics. However, they may be shifted too far towards the present, depending on whether potentially longer faecal shedding is real-

Figure 4: Reproductive number estimates. The different colours show estimates based on wastewater influenza measurements (blue) and laboratory-confirmed influenza cases (red). Coloured bands show the combined 95% bootstrap confidence and 95% credible intervals for each estimate (see the Methods for details). Shaded areas show when work-from-home measures were in place (see table 1). IAV: influenza A virus.

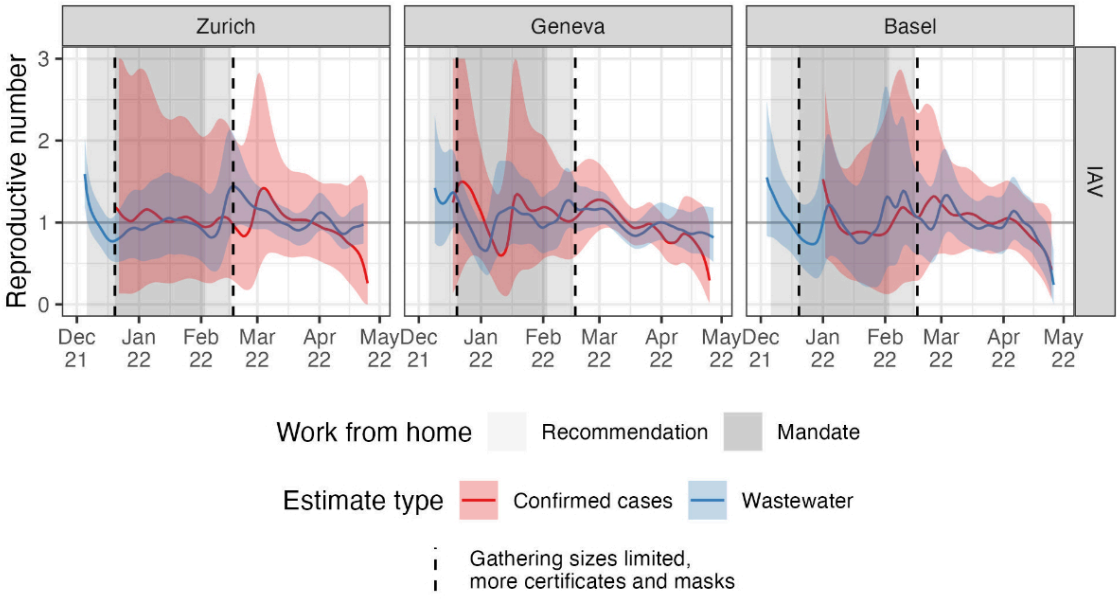

ly the primary driver of wastewater influenza loads (figure S4). We justify using a respiratory shedding load distribution here by noting that respiratory shedding appears to be orders of magnitude greater than faecal shedding (figure S8 in the appendix) [25–26, 34–35]. We also note that trends in wastewater-based infection incidence align better with confirmed case-based estimates when assuming a respiratory shedding load distribution (figure 3 and figure S4 in the appendix). However, the timeline of these case-based estimates was also subject to our assumption of a delay distribution based on symptom severity over time. Therefore, we cannot make concrete statements on the lead or lag times between wastewater and case-based indicators of influenza incidence. We plan to update the shedding load and time-to-case-confirmation distributions used in our accompanying dashboard should more data become available.

This project highlights the potential of wastewater-based surveillance for generating public health-relevant insights beyond SARS-CoV-2. Namely, we showed that wastewater measurements were more sensitive to a peak in influenza A virus incidence in Switzerland in December 2021 than confirmed case data or syndromic surveillance data on influenza-like illnesses. Wastewater data also yielded more precise R_e estimates than confirmed case data on the same geographic scale (catchment areas). The Federal Office of Public Health noted in its 2021/22 influenza season report that COVID-19 measures "most likely" reduced influenza transmission in Switzerland [28]. Our wastewater-based results provide additional evidence of a correspondence between influenza transmission (quantified by estimated infection incidence and R_e) and mobility restriction measures in response to COVID-19.

To our knowledge, this is the first time a mechanistic model has been applied to quantify influenza transmission dynamics from wastewater data. We emphasize that the development of mechanistic models for wastewater-based epidemiology is still in its infancy. Such models could, in principle, incorporate both clinical/syndromic surveillance and wastewater data simultaneously and more detailed assumptions on noise-generating processes. Methodological developments along these lines should improve the robustness and precision of wastewater-based estimates for pathogen transmission dynamics.

A prerequisite for applying complicated mechanistic models is a robust pathogen quantification method for wastewater. Our data are based on flow-normalized loads from raw wastewater influent quantified using either RT-qPCR or RT-dPCR. Despite considerable temporal variation in load measurements (figure 2A), both methods were sufficient for estimating infection incidence and R_e over the course of a flu season. There are many alternative approaches for sampling and quantifying human viruses in wastewater, including using settled solids rather than raw influent (e.g. Boehm et al. [7]) or alternative normalization approaches, such as normalization by pepper mild mottle virus. Any improvement in quantification accuracy would be expected to reduce uncertainty in estimated infection incidence and R_e. We note that R_e is a particularly convenient metric for wastewater pathogen surveillance because it is based on relative changes over time. Therefore, it is robust to different quantification methods provided quantification sensitivity is constant over time and most measurements exceed the detection limit. For example, Huisman et al. [19] showed that R_e estimation for SARS-CoV-2 was possible from both raw influent and settled solids. We anticipate our approach for influenza R_e estimation is similarly adaptable.

We have continued to measure influenza A and influenza B virus loads in Swiss wastewater since October 2022 and generate corresponding estimates for infection incidence and the effective reproductive number by catchment area. These results are available on an online dashboard at https://wise.ethz.ch/influenza/. We have made all the code for the analysis and this dashboard available on our project repository at https://github.com/wise-ch/wastewater-influenza-dashboard. We envision these results will help improve influenza surveillance in Switzerland by serving as an alternate source of information that is less susceptible to some case-based surveillance challenges amplified by the COVID-19 pandemic. More generally, we envision that our surveillance dashboard and the open-source code supporting it can serve as a blueprint for international surveillance efforts. Finally, as we generate more seasons of high-quality wastewater data and develop detailed mechanistic models, we expect to move beyond surveillance to generate new insights on the drivers of influenza transmission based on wastewater data.

Data and code availability

The catchment-level wastewater load and confirmed case data used in this manuscript are available along with the code at the project repository at https://github.com/wise-ch/wastewater-influenza-dashboard. Specifically, the wastewater load data (before normalization by the minimum detected load) and confirmed case data are available in the files prefixed "clean_data_" at https://github.com/wise-ch/wastewater-influenza-dashboard/tree/master/data/data_used_in_manuscript. A study protocol has not been prepared.

Acknowledgments

We are grateful to the many individuals who helped with this project. Taru Singhal provided code upon which the dashboard shiny app is based. Adrian Lison helped set up and maintain the dashboard. Charlie Gan, Franziska Böni, Laura Brülisauer, Camila Morales Undurraga, Johannes Rusch, and Lea Caduff processed wastewater samples. We thank the employees of the wastewater treatment plants ProRheno AG (Basel), ARA Werdhölzli (Zurich), and STEP d'Aïre (Geneva), for providing samples. Finally, the Swiss Federal Office of Public Health provided confirmed case data that was reported under the obligatory reporting system in Switzerland.

Financial disclosure

We gratefully acknowledge funding support from the Swiss Federal Office of Public Health and a Swiss National Science Foundation Sinergia grant number CRSII5_205933.

Potential competing interests

All authors have completed and submitted the International Committee of Medical Journal Editors form for disclosure of potential conflicts of interest. Tanja Stadler is a member of the scientific advisory board COVID-19 to the Swiss government. No other potential conflict of interest related to the content of this manuscript was disclosed.

References

1. WHO. (2014). "Global Influenza Programme". https://www.who.int/teams/global-influenza-programme/surveillance-and-monitoring

2. CDC. (2022). "2021-2022 U.S. Flu Season: Preliminary In-Season Burden Estimates". https://www.cdc.gov/flu/about/burden/preliminary-in-season-estimates.htm
3. WHO. (2013). "Global Epidemiological Surveillance Standards for Influenza". https://www.who.int/publications/i/item/9789241506601
4. WHO. (2022). "Guidelines for the clinical management of severe illness from influenza virus infections". https://apps.who.int/iris/handle/10665/352453
5. CDC. (2022). "Similarities and Differences between Flu and COVID-19 | CDC". https://www.cdc.gov/flu/symptoms/flu-vs-covid19.htm
6. Dhanasekaran, V., Sullivan, S., Edwards, K.M., Xie, R., Khvorov, A., Valkenburg, S.A., Cowling, B.J., Barr, I.G. (2022). Human seasonal influenza under COVID-19 and the potential consequences of influenza lineage elimination. Nature Communications 2022 13:1 13, 1–11. doi: http://dx.doi.org/10.1038/s41467-022-29402-5.
7. Boehm AB, Hughes B, Duong D, Chan-Herur V, Buchman A, Wolfe MK, et al. Wastewater concentrations of human influenza, metapneumovirus, parainfluenza, respiratory syncytial virus, rhinovirus, and seasonal coronavirus nucleic-acids during the COVID-19 pandemic: a surveillance study. Lancet Microbe. 2023 May;4(5):e340–8. http://dx.doi.org/10.1016/S2666-5247(22)00386-X.
8. FOPH. (2022). "Saisonale Grippe – Lagebericht Schweiz". https://www.bag.admin.ch/bag/de/home/krankheiten/ausbrueche-epidemien-pandemien/aktuelle-ausbrueche-epidemien/saisonale-grippe---lagebericht-schweiz.html
9. WHO. (2022). "Influenza Update No. 427". https://www.who.int/publications/m/item/influenza-update-n-427
10. Fernandez-Cassi X, Scheidegger A, Bänziger C, Cariti F, Tuñas Corzon A, Ganesanandamoorthy P, et al. Wastewater monitoring outperforms case numbers as a tool to track COVID-19 incidence dynamics when test positivity rates are high. Water Res. 2021 Jul;200:117252. http://dx.doi.org/10.1016/J.WATRES.2021.117252. http://dx.doi.org/10.1016/j.watres.2021.117252.
11. Xagoraraki I, O'Brien E. Wastewater-Based Epidemiology for Early Detection of Viral Outbreaks. In: O'Bannon DJ, editor. Women in Water Quality, Women in Engineering and Science. Springer Nature Switzerland AG; 2020. pp. 75–97. http://dx.doi.org/10.1007/978-3-030-17819-2_5.
12. Kilaru P, Hill D, Anderson K, Collins MB, Green H, Kmush BL, et al. Wastewater Surveillance for Infectious Disease: A Systematic Review. Am J Epidemiol. 2022; http://dx.doi.org/10.1093/AJE/KWAC175. http://dx.doi.org/10.1093/aje/kwac175.
13. Medema G, Been F, Heijnen L, Petterson S. Implementation of environmental surveillance for SARS-CoV-2 virus to support public health decisions: Opportunities and challenges. Current Opinion in Environmental Science and Health. Volume 17. Elsevier B.V.; 2020. pp. 49–71. http://dx.doi.org/10.1016/j.coesh.2020.09.006.
14. Wolfe MK, Duong D, Bakker KM, Ammerman M, Mortenson L, Hughes B, et al. Wastewater-Based Detection of Two Influenza Outbreaks. Environ Sci Technol Lett. 2022;9(8):687–92. http://dx.doi.org/10.1021/acs.estlett.2c00350.
15. Mercier E, Aoust PM, Thakali O, Hegazy N, Jia JJ, Zhang Z, et al. (2022). Wastewater surveillance of influenza activity: Early detection, surveillance, and subtyping in city and neighbourhood communities. MedRxiv, 2022.06.28.22276884. https://doi.org/ http://dx.doi.org/10.1101/2022.06.28.22276884.
16. Ort C, van Nuijs AL, Berset JD, Bijlsma L, Castiglioni S, Covaci A, et al. Spatial differences and temporal changes in illicit drug use in Europe quantified by wastewater analysis. Addiction. 2014 Aug;109(8):1338–52. http://dx.doi.org/10.1111/add.12570.
17. Julian T, Ort C, Caduff L, Gan C, Rusch J, Böni F, et al. (2020). "SARS-CoV-2 in Wastewater" https://www.eawag.ch/en/department/sww/projects/sars-cov2-in-wastewater/
18. Bagutti, C., Alt Hug, M., Heim, P., Maurer Pekerman, L., Ilg Hampe, E., Hübner, P., Fuchs, S., Savic, M., Stadler, T., Topolsky, I., Icer Baykal, P., Dreifuss, D., Beerenwinkel, N., & Tschudin Sutter, S. (2022). Wastewater monitoring of SARS-CoV-2 shows high correlation with COVID-19 case numbers and allowed early detection of the first confirmed B.1.1.529 infection in Switzerland: results of an observational surveillance study. Swiss Medical Weekly 2022 :25, 152(25), w30202. https://doi.org/ http://dx.doi.org/10.4414/SMW.2022.W30202. http://dx.doi.org/10.4414/SMW.2022.w30202.
19. Huisman JS, Scire J, Caduff L, Fernandez-Cassi X, Ganesanandamoorthy P, Kull A, et al. Wastewater-Based Estimation of the Effective Reproductive Number of SARS-CoV-2. Environ Health Perspect. 2022 May;130(5):57011. http://dx.doi.org/10.1289/ehp10050. http://dx.doi.org/10.1289/EHP10050.
20. Scire J, Huisman JS, Grosu A, Angst DC, Li J, Maathuis MH, et al. (2022). estimateR: An R package to estimate and monitor the effective reproductive number. MedRxiv, 2022.06.30.22277095. https://doi.org/ http://dx.doi.org/10.1101/2022.06.30.22277095.
21. Cori A, Ferguson NM, Fraser C, Cauchemez S. A new framework and software to estimate time-varying reproduction numbers during epidemics. Am J Epidemiol. 2013 Nov;178(9):1505–12. http://dx.doi.org/10.1093/aje/kwt133.
22. Wade MJ, Lo Jacomo A, Armenise E, Brown MR, Bunce JT, Cameron GJ, et al. Understanding and managing uncertainty and variability for wastewater monitoring beyond the pandemic: lessons learned from the United Kingdom national COVID-19 surveillance programmes. J Hazard Mater. 2022 Feb;424 Pt B:127456. http://dx.doi.org/10.1016/j.jhazmat.2021.127456.
23. Zahedi A, Monis P, Deere D, Ryan U. Wastewater-based epidemiology-surveillance and early detection of waterborne pathogens with a focus on SARS-CoV-2, Cryptosporidium and Giardia. Parasitol Res. 2021 Dec;120(12):4167–88. http://dx.doi.org/10.1007/s00436-020-07023-5.
24. Carrat F, Vergu E, Ferguson NM, Lemaitre M, Cauchemez S, Leach S, et al. Time lines of infection and disease in human influenza: a review of volunteer challenge studies. Am J Epidemiol. 2008 Apr;167(7):775–85. http://dx.doi.org/10.1093/aje/kwm375.
25. Hirose R, Daidoji T, Naito Y, Watanabe Y, Arai Y, Oda T, et al. Long-term detection of seasonal influenza RNA in faeces and intestine. Clin Microbiol Infect. 2016 Sep;22(9):813.e1–7. http://dx.doi.org/10.1016/j.cmi.2016.06.015.
26. Chan MC, Lee N, Chan PK, To KF, Wong RY, Ho WS, et al. Seasonal influenza A virus in feces of hospitalized adults. Emerg Infect Dis. 2011 Nov;17(11):2038–42. http://dx.doi.org/10.3201/eid1711.110205.
27. Ferguson, N. M., Cummings, D. A. T., Cauchemez, S., Fraser, C., Riley, S., Meeyai, A., Iamsirithaworn, S., & Burke, D. S. (2005). Strategies for containing an emerging influenza pandemic in Southeast Asia. Nature 2005 437:7056, 437(7056), 209–214. https://doi.org/ http://dx.doi.org/10.1038/nature04017.
28. FOPH. (2022). "Bericht zur Grippesaison 2021/22" https://www.bag.admin.ch/dam/bag/de/dokumente/mt/infektionskrankheiten/grippe/saison-bericht-grippe-2021-22.pdf.download.pdf/saisonbericht-grippe-2021-22_DE.pdf
29. Borchers H. (2022). pracma: Practical Numerical Math Functions. R package version 2.4.2, https://CRAN.R-project.org/package=pracma
30. FOPH. (2022). "Coronavirus: Measures and Ordinances." https://www.bag.admin.ch/bag/en/home/krankheiten/ausbrueche-epidemien-pandemien/aktuelle-ausbrueche-epidemien/novel-cov/massnahmen-des-bundes.html
31. SWI. (2022). "Coronavirus: The Situation in Switzerland". https://www.swissinfo.ch/eng/society/covid-19_coronavirus--the-situation-in-switzerland/45592192
32. Federal Council. (2022). "Coronavirus: Federal Council to lift measures – mask requirement on public transport and in healthcare institutions and isolation in the event of illness to remain until end of March". https://www.admin.ch/gov/en/start/documentation/media-releases.msg-id-87216.html
33. Brugger J, Althaus CL. Transmission of and susceptibility to seasonal influenza in Switzerland from 2003 to 2015. Epidemics. 2020 Mar;30:100373. http://dx.doi.org/10.1016/j.epidem.2019.100373.
34. Lau LL, Cowling BJ, Fang VJ, Chan KH, Lau EH, Lipsitch M, et al. Viral shedding and clinical illness in naturally acquired influenza virus infections. J Infect Dis. 2010 May;201(10):1509–16. http://dx.doi.org/10.1086/652241.
35. To KK, Chan KH, Li IW, Tsang TY, Tse H, Chan JF, et al. Viral load in patients infected with pandemic H1N1 2009 influenza A virus. J Med Virol. 2010 Jan;82(1):1–7. http://dx.doi.org/10.1002/jmv.21664.
36. Integrated DN. Technologies. (n.d.). 2019-nCoV Research Use Only qPCR Probe Assay primer/probe mix. Retrieved December 5, 2022, from https://sfvideo.blob.core.windows.net/sitefinity/docs/default-source/supplementary-product-info/supplemental-information---2019-ncov-assay---ruo.pdf?sfvrsn=2bcf1507_2
37. Ward CL, Dempsey MH, Ring CJ, Kempson RE, Zhang L, Gor D, et al. Design and performance testing of quantitative real time PCR assays for influenza A and B viral load measurement. J Clin Virol. 2004 Mar;29(3):179–88. http://dx.doi.org/10.1016/S1386-6532(03)00122-7.
38. Fry AM, Chittaganpitch M, Baggett HC, Peret TC, Dare RK, Sawatwong P, et al. The burden of hospitalized lower respiratory tract infection due to respiratory syncytial virus in rural Thailand. PLoS One. 2010 Nov;5(11):e15098. http://dx.doi.org/10.1371/journal.pone.0015098.

Appendix

Supplemental methods

RT-dPCR procedure

Pathogen RNA quantification was done for samples from the Zurich and Geneva facilities using digital reverse transcription PCR (RT-dPCR) on the Crystal Digital PCR Naica System (Stilla Technologies, France) with qScript XLT One-Step RT-qPCR Kit (CN: 95132-02K, Quantabio, MA, USA). Two assays were used, IABV and RESPV4. IABV is a duplex assay with IAV and IBV, targeting the matrix proteins of each respective virus (figure S11). RESPV4 is an updated tetraplex assay that incorporates SARS-CoV-2 Nucleoprotein locus 2 (N2) and Respiratory Syncytial Virus Matrix protein (RSV), while including the aforementioned IAV and IBV targets (figure S11). The mastermix final volume was 27 µl, with 5.4 µl of template and 21.6 µl of pre-mix. The premix consists of the US CDC SARS-CoV-2 RUO Kit N2, with a primer and probe final concentration of 500 nM and 125 nM, respectively [36] (Integrated DNA Technologies, USA). IAV, IBV and RSV all had primers at a final concentration of 500 nM. The RSV probe had a final concentration of 400 nM, and the IAV and IBV probes were at a final concentration of 200 nM. Fluorescein was added at a final concentration of 125 nM as a background dye for droplet detection. Finally, RNAse/DNAse-free water was added (variable, depending on stock concentrations) to bring the pre-mix to the correct final volume, of which 25 µL was pipetted into Sapphire Chips (Stilla Technologies). Thermocycling conditions included droplet partitioning at 40 ºC for 12 minutes, followed by reverse transcription at 50 ºC for 1 hour, and then followed by 40 cycles of 95 ºC for 30 s and 57.5 ºC for 60 s. Chips were subsequently read on the Stilla Prism3 chip reader for the IABV assay or the Stilla Prism6 chip reader for the RESPV4 assay.

Analysis of IAV included results from both IABV and RESPV4, whereas with IBV only the measurements for RESPV4 were used due to insufficient separation of positive droplets (figure S9). Samples were run in technical duplicate, and each measurement consisted of 23’648 droplets on average, with a standard deviation of 6’628 droplets. Each droplet is assumed to have a volume of 519 nL. Measurements were only included if they had at least 15’000 droplets. Droplets of incorrect volume (polydispersity) if present were manually excluded from the analysis. Quality control included one no-template control and one positive control with every five samples, and inhibition testing for the SARS-CoV-2 N1 locus for every sample as previously described. Positive controls are shown in figures S9 and S10.

Delay distributions

For the delay between infection and respiratory shedding and the delay between infection and symptoms, we used the distributions given in Carrat et al. [24]. We assumed that this second distribution (infection to symptoms) is a good approximation for the delay between infection and an individual getting a diagnostic test. To generate gamma distributions from the data presented in Carrat et al. [24], we digitized figure 2 from that paper using the online tool https://automeris.io/WebPlotDigitizer/. We then matched a gamma distribution to the digitized data by calculating the mean and standard deviation of the empirical distributions of the two types of data. We used these means and standard deviations for our gamma delay distributions. Figure S1A and S1C show the correspondence between the Carrat et al. data [24] and the fitted distributions. For the delay between infection and fecal shedding we collated data from two previously published studies [25-26]. These included at least one patient with IBV infection, but were primarily from patients with IAV infection. We shifted the data by two days to account for the fact that measurement days were relative to symptom onset, based on an average delay from infection to symptom onset of 2 days given in Carrat et al. [24]. We calculated the mean viral concentration by day and matched a gamma distribution to these values using the moments of the empirical data distribution as above. Figure S1B shows the correspondence between the data and the fitted distribution.

Figure S1: Delay distributions used to reconstruct infection incidence. (A) shows the delay distribution used for infection to a diagnostic test. (B) shows the fecal shedding load distribution. Measurements were taken with reference to the date of symptom onset, so here they are shifted two days to account for an assumed 2-day fixed delay between infection and symptom onset. One outlier measurement of 4639335 is not shown in this plot but was used for fitting the gamma distribution. (C) shows the respiratory shedding load distribution.

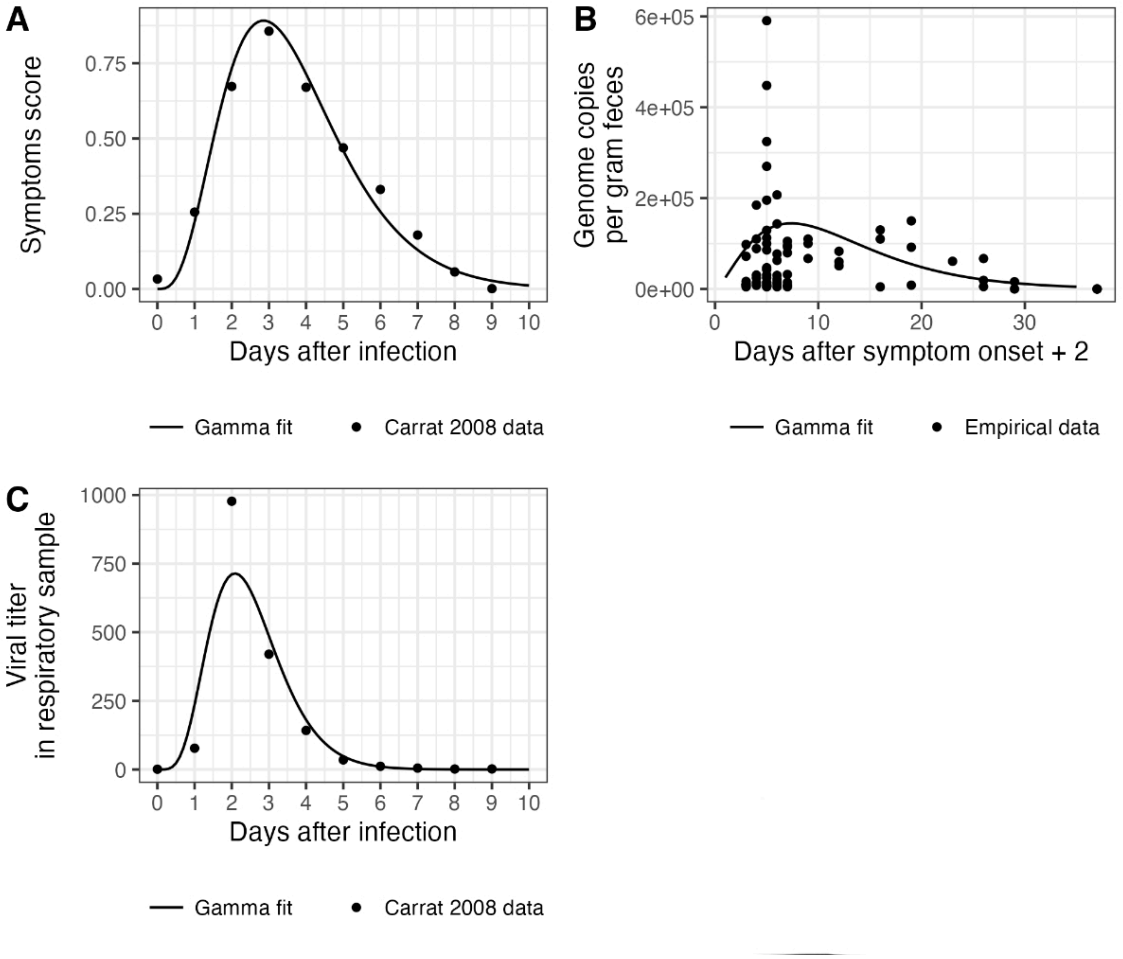

Figure S2: Raw wastewater influenza measurements. Each open point represents a unique measurement. Measurements from the same catchment on the same day are replicate measurements based on multiple aliquots. We use data generated using three different assays, which are shown in different colours.

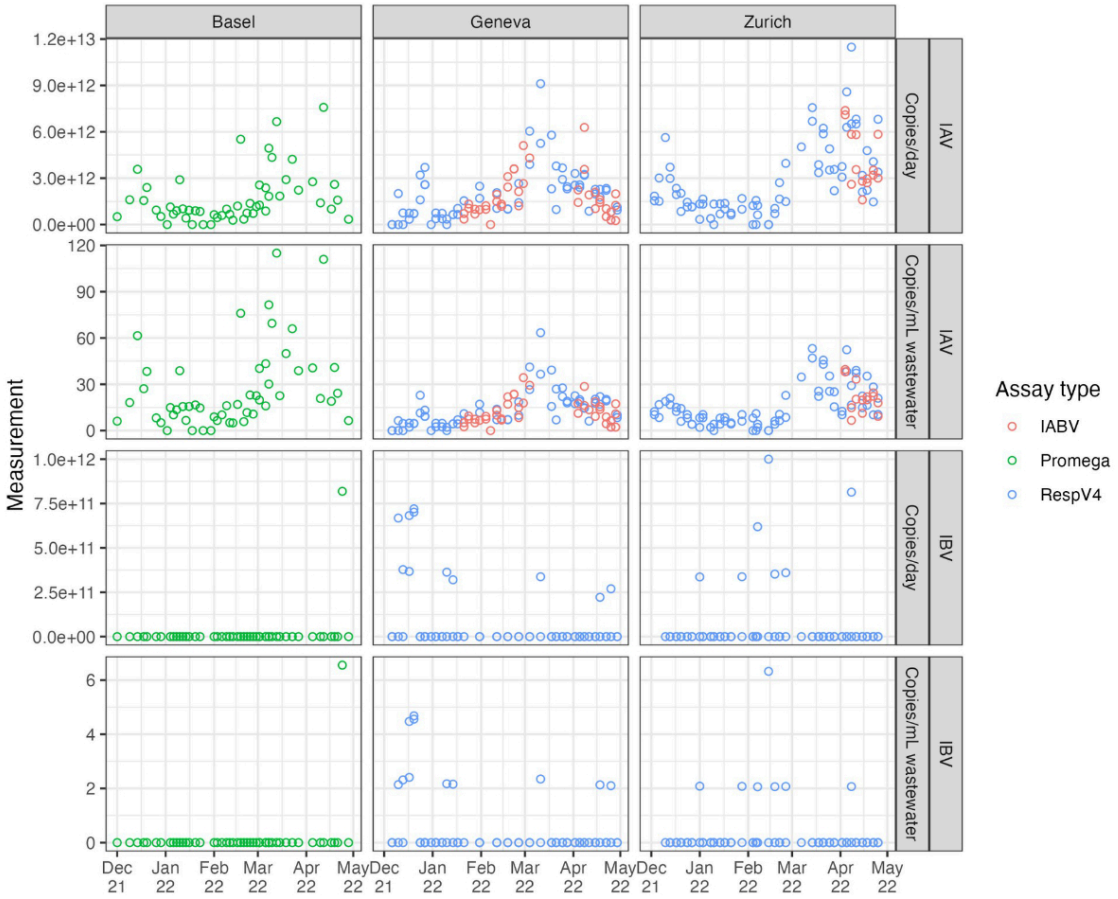

Figure S3: Input data for Re estimation. Cases are laboratory-confirmed influenza infections (by catchment area, reported weekly). Wastewater input data are virus load (genome copies per day) scaled by the minimum non-zero measurement for the respective wastewater treatment plant. The points show the actual data, and the lines show the cubic spline interpolation used to generate daily values for Re estimation.

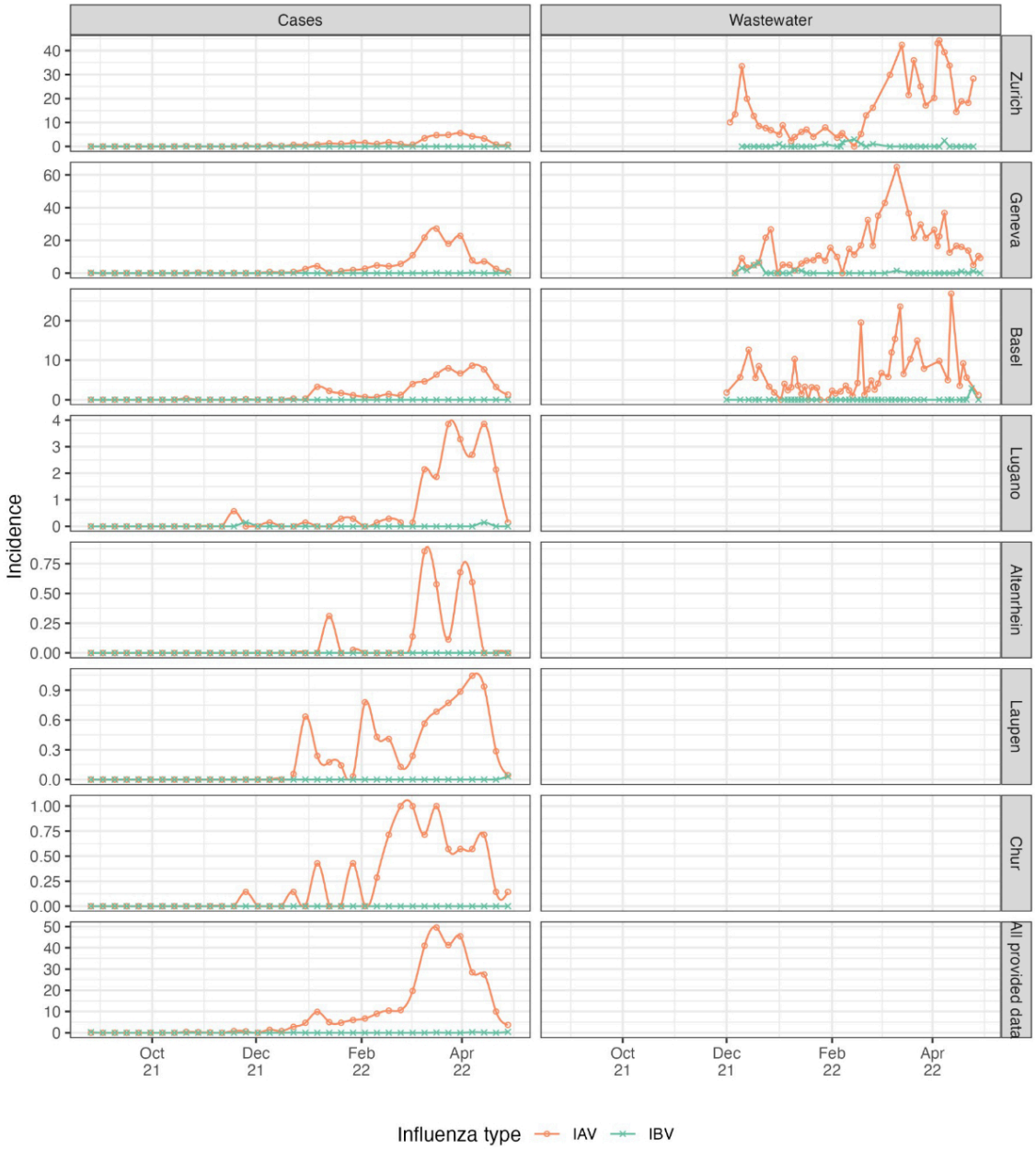

Figure S4: Sensitivity analysis for the delay distribution. We used two different shedding load distributions to deconvolve wastewater influenza measurements to infection incidence, one based on measurements of influenza in the stool ("Fecal") and one based on measurements of influenza shedding from the respiratory tract ("Respiratory"). The two distributions are shown in figure S3. (A) The infection incidence estimates using each distribution, and (B) the reproductive number estimates. The thicker grey horizontal line in (B) shows the epidemic threshold at a reproductive number of 1. The shaded grey rectangles highlight periods when work-from-home measures were in place.

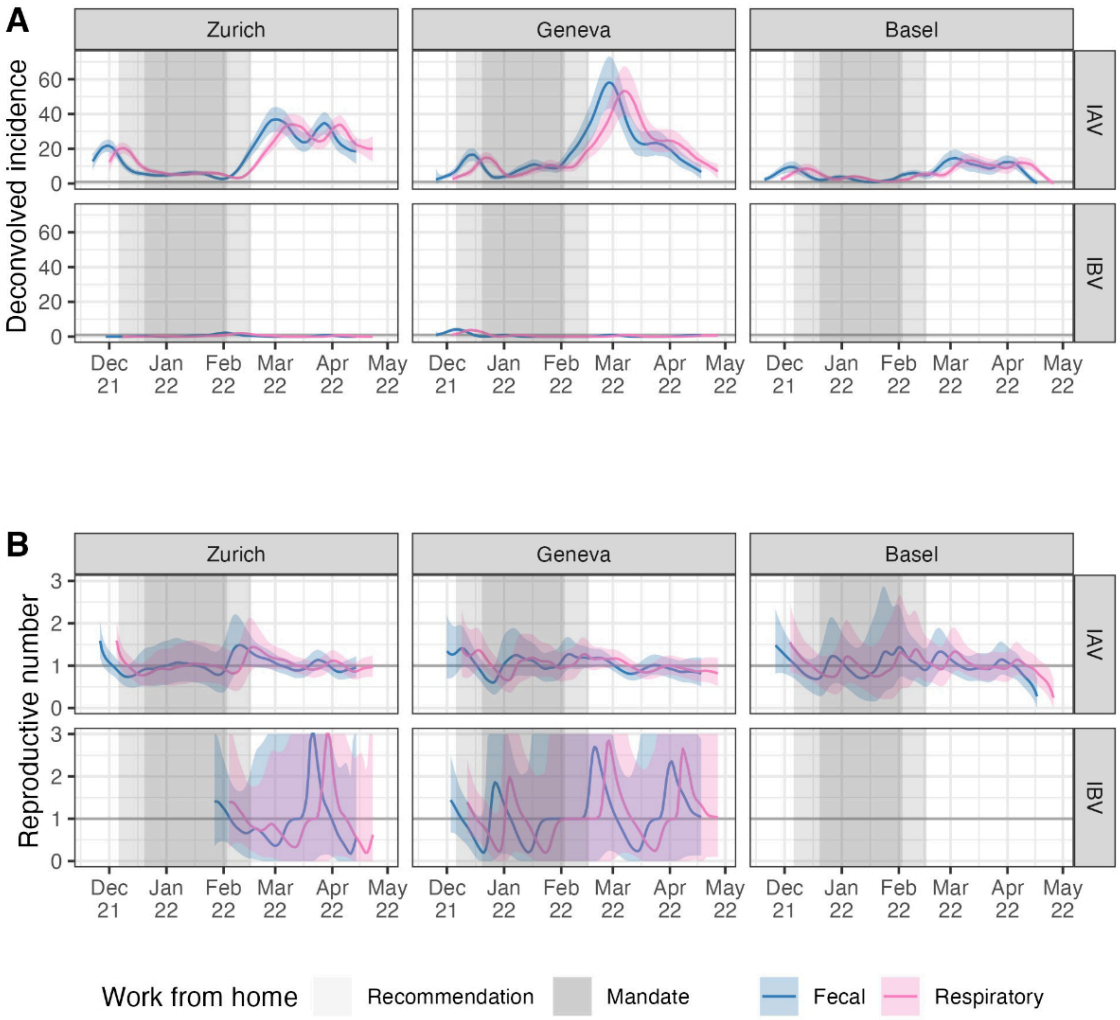

Figure S5: Sensitivity analysis for wastewater measurement scaling. Results are based on the same wastewater loads for IAV from the Zurich catchment but scaled so that the minimum detected load corresponds to 1, 10, 100, or 1000 assumed cases in the catchment area.

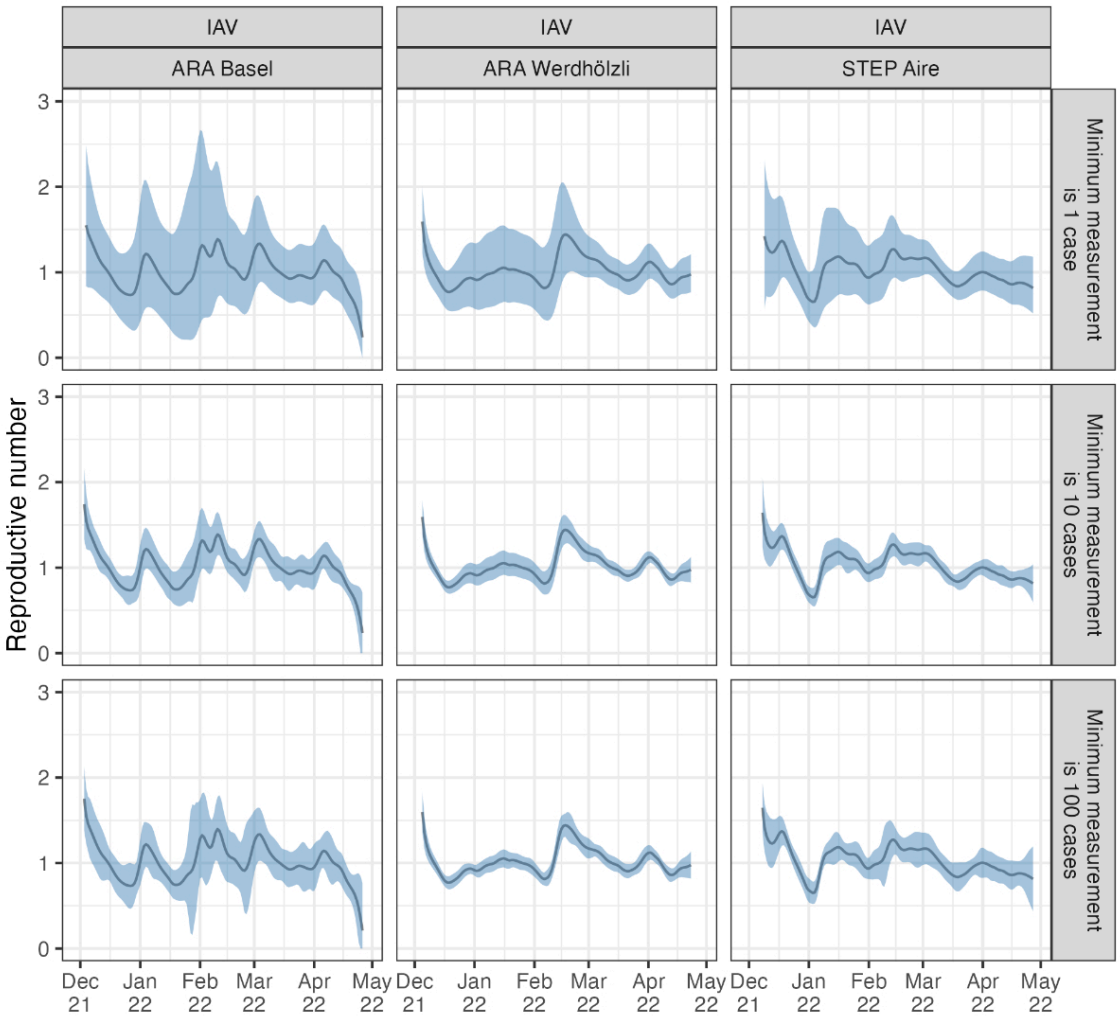

Figure S6: Reproductive number estimates for six different catchment areas and all postal codes for which we have case data. Results are not shown when the cumulative number of deconvolved cases is below 12, which was the case for the influenza B virus for most case-based data and for the influenza A virus in the case data from the Altenrhein catchment area. The thicker grey horizontal line shows the epidemic threshold at a reproductive number of 1.

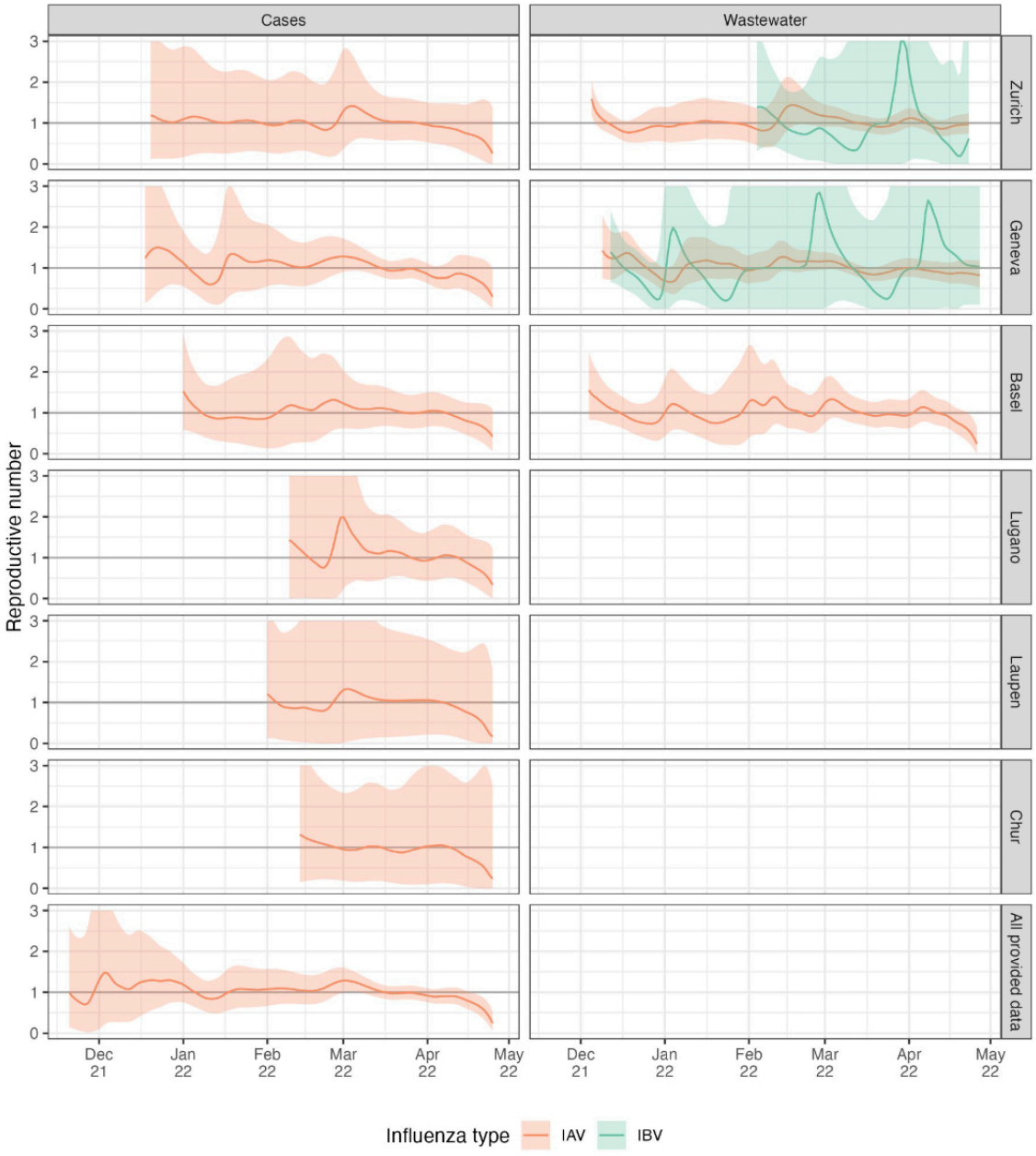

Figure S7: Screenshot of 2022/23 influenza Re results. Ongoing surveillance results are available at the website https://wise.ethz.ch/influenza/.

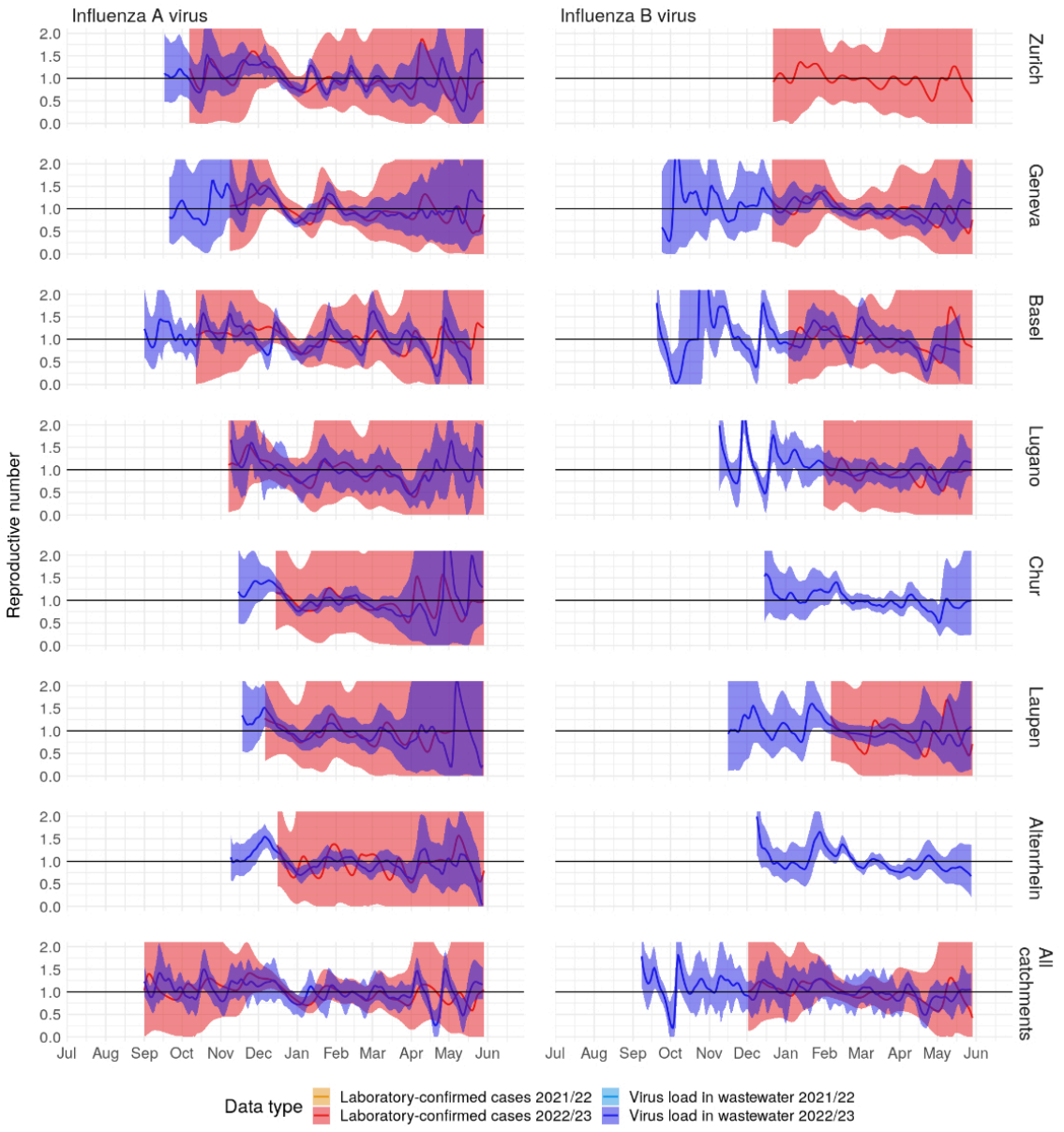

Figure S8: Influenza shedding measurements from a convenience sample of previous studies. “Respiratory” samples include nose-throat swabs and sputum. “Stool” samples are faeces. The referenced studies are Chan et al. [26], Hirose et al. [25], Lau et al. [34], and To et al. [35].

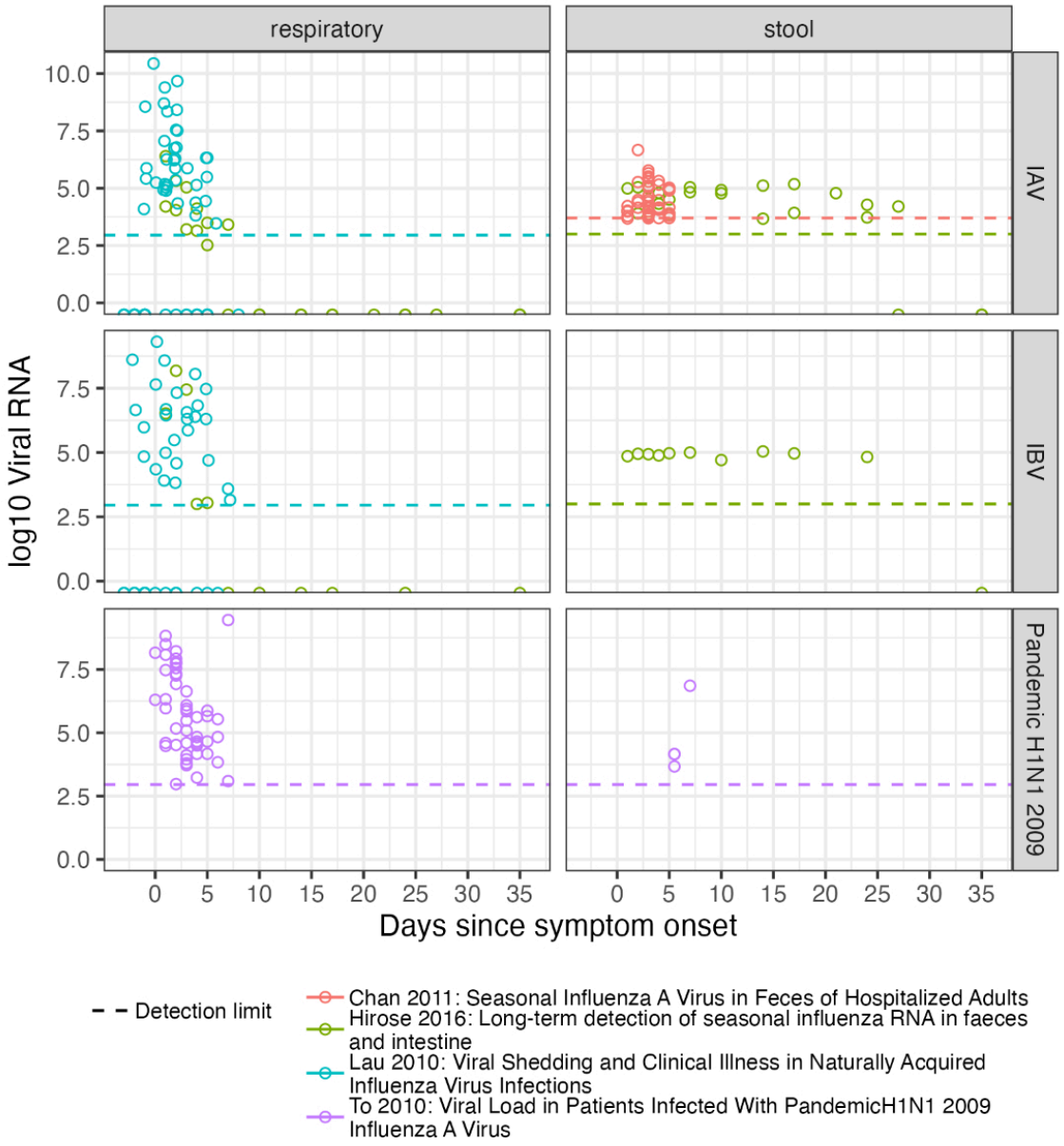

Figure S9: Gating of positive control samples for the assay “IABV”. The green fluorophore (y-axis) represents the IBV, and the red fluorophore (x-axis) represents the IAV. The rectangles show the fluorescence thresholds used to determine which droplets in samples were positive for each virus. This assay was only used to quantify IAV because there was no clear separation between positive and negative droplets for the IBV control.

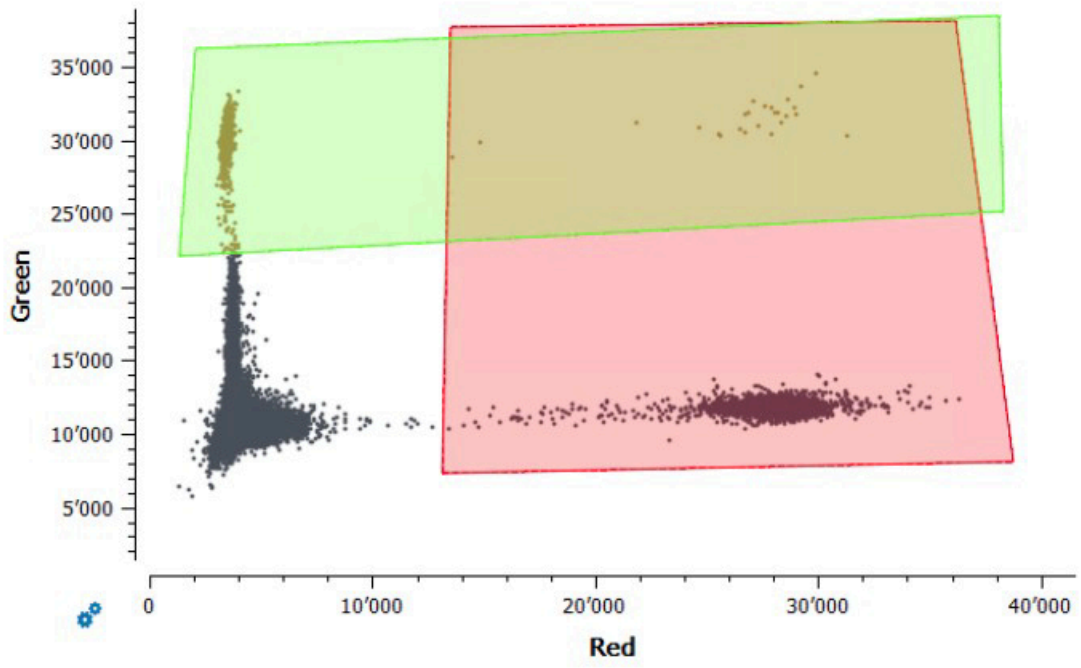

Figure S10: Gating of positive control samples for the assay “RESPV4”. The green and red fluorophores are for IBV and IAV, respectively, as for the assay “IABV”. The yellow and blue fluorophores are for respiratory syncytial virus (RSV) and SARS-CoV-2, respectively. The rectangles show the fluorescence thresholds used to determine which droplets in samples were positive for each virus.

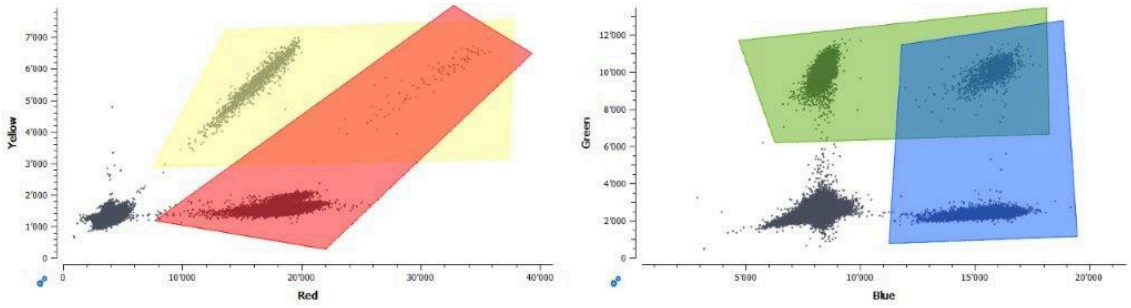

Figure S11: Primer and probe sequences. The primers and probes shown were used in the duplex (IABV) and tetraplex (RESPV4) assays for Zurich and Geneva wastewater treatment facilities. Sequences are in the 5' to 3' direction.

Target	Name	Sequence (5' →3')	Sense (+/-)	Amplicon Size (bp)	Final Assay Conc. (nM)	Reference
Influenza A (IABV, RESPV4) Matrix protein gene (M)	IAV-M_Neo_Fwd	TGG AAT GGC TAA AGA CAA GAC CAA T	+	110	500	Modified from Ward et al. 2004 [37]
	IAV-M_Neo_Rev	AAA GCG TCT ACG CTG CAG TCC	-		500	
	IAV-M_Neo_Probe	Cy5/TTT GTK TTC ACG CTC ACC GTG CCC/BHQ2	+		200	
Influenza B (IABV, RESPV4) Matrix protein gene (M)	IBV-M_Neo_Fwd	GAG ACA CAA TTG CCT ACY TGC TT	+	96	500	Modified from Ward et al. 2004 [37]
	IBV-M_Neo_Rev	ATT CTT TCC CAC CRA ACC AAC A	-		500	
	IBV-M_Neo_Probe	HEX/AGA AGA TGG AGA AGG CAA AGC AGA ACT AGC/BHQ2	+		200	
SARS-CoV-2 (RESPV4) Nucleoprotein gene locus 2 (N2)	2019-nCoV-N2-F	TTA CAA ACA TTG GCC GCA AA	+	67	500	SARS-CoV-2 RUO qPCR Primer & Probe Kit (IDT)
	2019-nCoV-N2-R	GCG CGA CAT TCC GAA GAA	-		500	
	2019-nCoV-N2-P	FAM/ACA ATT TGC CCC CAG CGC TTC AG/BHQ1	+		125	
Respiratory Syncytial Virus (RESPV4) Matrix protein gene (M)	RSV_Metavir_Fwd	GGC AAA TAT GGA AAC ATA CGT GAA	+	117	500	Modified from Fry et al. 2010 [38]
	RSV_Metavir_Rev	GGC ACC CAT ATT GTW AGT GAT G	-		500	
	RSV_Metavir_Probe	ATTO620/GCT GTG TAT GTG GAG CCY TCG TGA AG/BHQ2	-		400	